Applied Surface Science 258 (2012) 8475–8483

Contents lists available at SciVerse ScienceDirect

Applied Surface Science

journal homepage: www.elsevier.com/locate/apsusc

Time-resolved shadowgraph imaging of femtosecond laser-induced forward transfer of solid materials

M. Feinaeugle[a,*], A.P. Alloncle[b], Ph. Delaporte[b], C.L. Sones[a], R.W. Eason[a]

[a] Optoelectronics Research Centre, University of Southampton, Southampton, SO17 1BJ, UK
[b] LP3 laboratory, UMR7341 CNRS – Aix-Marseille University, 163 avenue de Luminy C.917, 13288 Marseille cedex 9, France

ARTICLE INFO

Article history:
Received 21 November 2011
Received in revised form 2 April 2012
Accepted 15 April 2012
Available online 31 May 2012

Keywords:
Laser-induced forward transfer
Shadowgraphy
Time-resolved studies
Femtosecond
Shock wave
Laser material processing

ABSTRACT

The transfer of solid phase material by femtosecond laser-induced forward transfer (LIFT) at atmospheric pressure by a time-resolved shadowgraph technique is studied. The influence of laser fluence on transfer of material in solid, fragmented and molten state is investigated during femtosecond LIFT of initially solid layers of thermoelectric bismuth selenide (Bi_2Se_3), piezoelectric lead zirconate titanate (PZT) and magnetostrictive Terfenol-D. We report ejection velocities of ~48 m/s and ~34 m/s for intact transfer of ~1.1 μm thick Bi_2Se_3 and ~1.8 μm thick PZT respectively, and of ~140 m/s for ~0.5 μm thick Terfenol-D. During intact transfer, contrary to what has been reported so far, no shock wave above the substrate surface was observed.

1. Introduction

Thin films deposited by laser-induced forward transfer (LIFT), a laser direct-write technique, find wide use in areas of electronics [1,2], photonics [3] and biotechnology [4,5]. The versatility and the simplicity of the LIFT process in addition to the absence of any lithographic process steps, make this technique a powerful tool for prototyping or repair [6].

The LIFT setup consists of a laser source, beam guiding optics and the sample assembly. During LIFT transfer the image of an aperture is projected or focussed at the interface between an optically transparent substrate (referred to as the carrier) and a thin layer of the material to be transferred (referred to as the donor). The donor-coated carrier (referred to as the target) is placed in proximity or in contact with the acceptor substrate (referred to as the receiver), which is facing the donor side of the LIFT target.

In order to further extend the applicability for LIFT, we have investigated its feasibility for transferring materials used for energy harvesting devices. The design of such devices requires a technique that permits the printing of solid materials in an intact state onto a broad range of temperature-sensitive receivers such as polymers. Most alternative manufacturing techniques employ high temperature steps which would not be suitable for printing onto such polymer substrates. Additionally, for manufacturing energy harvesting devices the LIFTed material's phase, structure and temperature should ideally not change during transfer. For materials with a defined domain or crystal orientation such as piezoelectric ceramics, there is the additional need to transfer material without increasing its temperature above the Curie point.

Furthermore, such harvesting devices also require good adhesion of the deposited material to the acceptor substrate and low damage of the receiver. During LIFT therefore, one of the main objectives is to preserve the integrity of the donor under transfer (referred to as the flyer), and to limit the flyer's velocity. Suppressing the creation of shock waves, usually generated during the LIFT process is a major concern too, as these shock waves may interact destructively with the flyer on reflection from the receiver placed nearby [7].

In this contribution we present femtosecond (fs) LIFT as a viable candidate for intact transfer without the need of an additional auxiliary layer (referred to as dynamic release layer or DRL [8]), which has been employed primarily for the purpose of transferring donors in an intact state. In fs-based material processing, the interaction time between the laser pulse and the material is too short to allow direct heat transfer to the lattice of the flyer and this consequently reduces the heat-affected zone when compared to nanosecond (ns) or picosecond (ps) LIFT making possible the transfer of materials without melting of a significant fraction of the flyer [9,10].

In order to achieve intact transfer, it is of major importance to observe the interaction of the laser pulse with the transferred

* Corresponding author. Tel.: +44 02380 59 9091; fax: +44 02380 59 3142.
E-mail address: mf2v09@orc.soton.ac.uk (M. Feinaeugle).

0169-4332/$ – see front matter © 2012 Elsevier B.V. All rights reserved.
http://dx.doi.org/10.1016/j.apsusc.2012.04.101

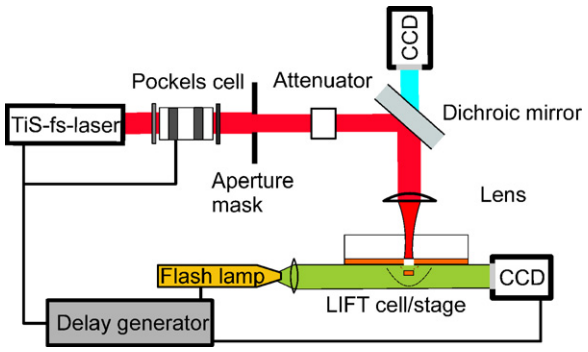

Fig. 1. Schematic of the experimental setup for shadowgraph studies of fs-LIFT.

material. The processes of material release and transfer during fs-LIFT were therefore investigated with a time-resolved shadowgraph imaging technique. This gives insight into the dynamics of material transfer and shows the interaction between the laser pulse, the donor and the surrounding atmosphere. We studied the transfer of a range of different donor materials such as thermoelectric bismuth selenide (Bi_2Se_3), piezoelectric lead zirconate titanate (PZT) and a magnetostrictive compound of terbium, dysprosium and iron (Terfenol-D). In the experiments, the flyer was imaged after a previously defined time delay following the absorption of the incident laser pulse by the donor. 'Transfer' in its real sense would have required the presence of a receiver. However, in the following, we may use the term transfer in order to emphasise the similarity and relevance of the observed ejection process to LIFT despite the absence of such a receiver.

So far the LIFT process has been investigated with time-resolved imaging techniques in the nanosecond [11,12] and sub-picosecond laser pulse range [13,14] for solid [15,16], powder [17] and liquid donors [18], and flyer velocity, shockwave creation and the interaction with the receiver have been investigated.

This study gives information about flyer velocity, and integrity during transfer, and the role of possible formation of shock waves. In this article we report the first shadowgraph imaging of intact solids under fs-LIFT using the shortest pulses used so far in time-resolved shadowgraph studies of LIFT.

2. Methods

The LIFT shadowgraph imaging experiments were carried out with the help of a femtosecond oscillator, and a chirped pulse amplification and compression laser system (Spectra-Physics Hurricane). The overall setup of the system can be seen in Fig. 1.

The laser emission wavelength was 800 nm and the pulse width was ~100 fs at full-width half maximum. The maximum energy per pulse reached 1 mJ at a repetition rate of 1 kHz. Single pulses were selected by a combination of a half-wave plate, a polariser and a Pockels cell which was driven by a pulse generator that was in turn synchronised with the amplifier stage of the laser system. Attenuation of the laser energy was effected with a polarising filter and a rotatable half-wave plate. A central part of the Gaussian beam profile was selected by a circular aperture and imaged onto the sample with the help of a plano-convex lens with a focal length of 50 mm. The resultant maximum pulse energy of ~15 μJ was imaged down at the carrier–donor interface to obtain a maximum energy density of ~3 J/cm^2 for a resultant flyer diameter of ~25 μm. The sample was positioned on a computer-controlled and motorised three-axis stage. A discharge flash lamp (HSPS Nanolite) was aligned to incoherently illuminate the sample so that the sample's surface was located at the object plane of a 100× infinity-corrected microscope objective. This imaging path was orthogonal to the direction of the incident femtosecond laser pulse. The images observed were captured on a high-speed CCD camera (Princeton Instruments) with a resolution of 1024 × 1024 pixels. The imaging system was setup in a way to achieve a compromise between a sufficiently large field of view and a simultaneous high magnification of the flyer. No receiver was used during the shadowgraph experiments in order to image a largest possible area above the donor surface.

All the different LIFT target films were prepared by sputtering onto 2 mm thick quartz substrates, with measured thicknesses of 1.1 μm for Bi_2Se_3 films, 0.5 μm for the layers of Terfenol-D and up to 1.8 μm for PZT films.

All the deposits were transferred via LIFT by single pulse exposure. The CCD camera and the flash lamp were synchronised so that the donor surface was illuminated at the same time as the camera shutter was opened. A signal generator delayed the image capturing in order to probe the donor surface at specific times after the interaction of the laser pulse with the donor. Images were captured with a delay time between 0 and 10 μs in order to time-resolve the evolution of the flyer movement away from the donor/carrier substrate. The illumination conditions depend on the flash duration of the Nanolite illumination system which was between 10 and 20 ns and had a random jitter of some tens of nanoseconds. All experiments were carried out under atmospheric pressure.

3. Results and discussion

First we investigated the transfer under different laser fluence regimes. From previous LIFT experiments we know that flyers are only released from the donor above a specific, incident laser fluence. For LIFT this laser threshold is not only a function of donor preparation and thickness, but is also a function of the laser pulse duration and wavelength, as it is for the case of laser ablation. [19]. It was of considerable practical interest to investigate conditions where the materials remained in solid phase during transfer as fragmented deposits would have limited applicability in the fabrication of our energy harvesting devices.

3.1. Bismuth selenide

The threshold fluence for the release of an intact flyer from a 1.1 μm thick bismuth selenide donor was ~90 ± 10 mJ/cm^2. The flyer for ~130 mJ/cm^2 was released in an intact state as well, while for ~400 mJ/cm^2 only fragments were ejected from the donor.

The shadowgraph images showing the transfer behaviour described are given in Fig. 2.

Fig. 2 shows the transfer of an intact flyer for a fluence of ~130 mJ/cm^2 which is slightly above transfer threshold (~90 mJ/cm^2) for LIFT of the Bi_2Se_3 donor used. The flyer remained intact for a travelled distance of ~250 μm. In more than 50% of the cases the flyer experienced a tilt from its initial orientation which was parallel to the donor surface. This was seen as a blurred or tilted flyer (delay times t = 2300 ns and t = 3800 ns in Fig. 2).

There was a clear qualitative and timing difference for material ejection between the transfers around the threshold fluence and a higher fluence. The earliest release of a flyer at threshold was seen at ~200–400 ns while for a higher fluence (~400 mJ/cm^2) particles emerged earlier, after ~50 ns, as shown in Fig. 3.

The most prominent difference seen under different fluence regimes was the appearance of intact flyers with low flyer velocities at threshold while multiple particles travelling at much faster velocities were ejected from the donor at higher fluences. In this latter case, after 250 ns, no further material from the donor was added to the particle cloud. However, the cloud kept expanding as its constituent elements travelled with different velocities. A particle's velocity normal to the donor surface was generally higher

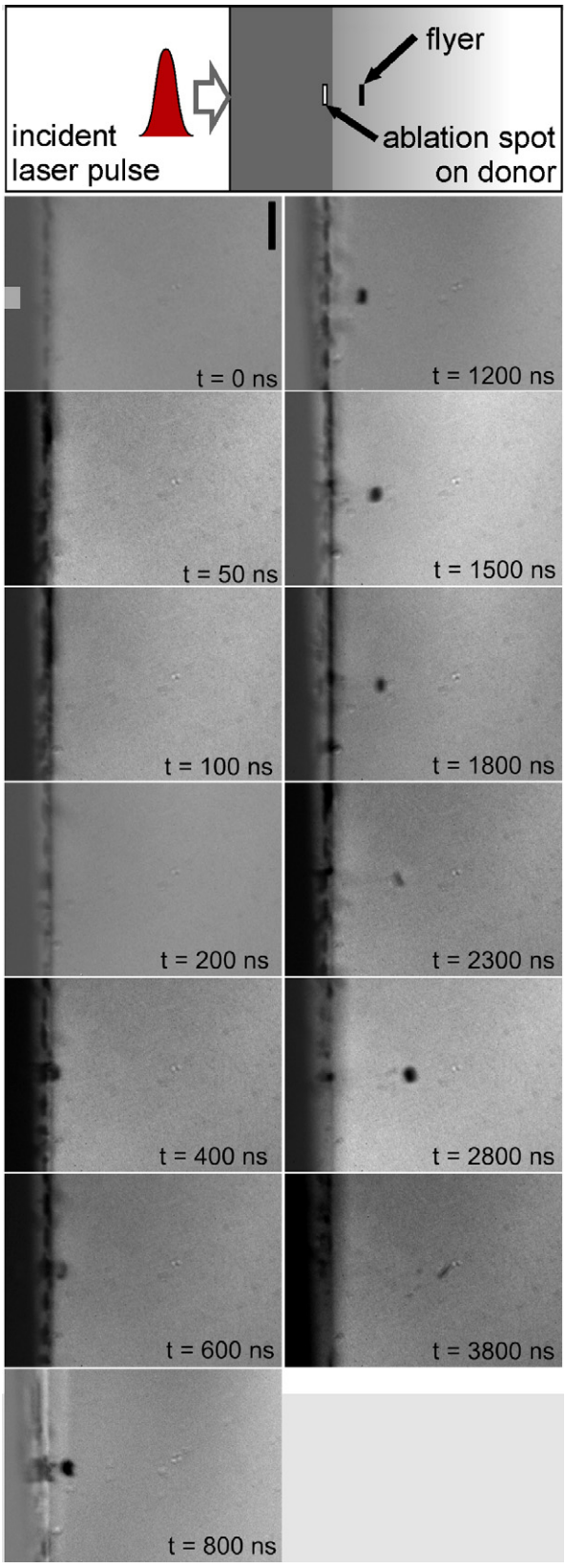

Fig. 2. Series of shadowgraph images of fs-LIFT of a Bi_2Se_3 flyer. Each frame was taken at a different camera delay time. The fluence used was ~130 mJ/cm^2. The scale bar in the first frame (t = 0 ns) is 100 μm wide, and the rectangle marks the approximate incident beam position.

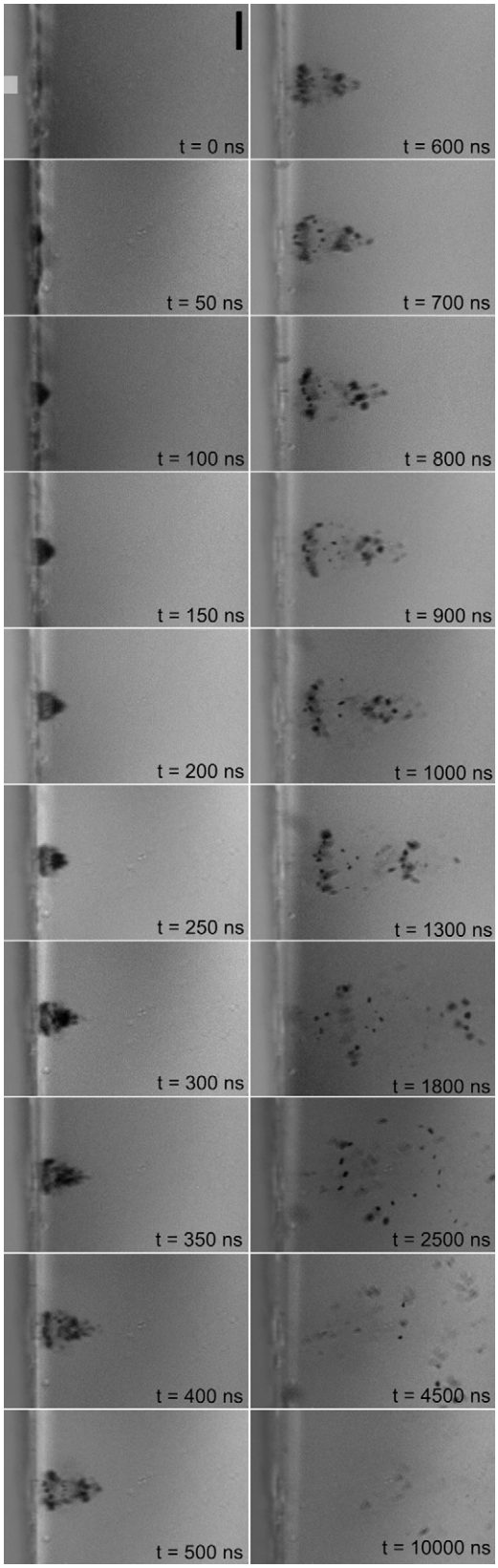

Fig. 3. Series of shadowgraph images of fs-LIFT of a Bi_2Se_3 flyer. Each frame was taken at a different camera delay time. The laser fluence was ~400 mJ/cm^2. The scale bar in the first frame (t = 0 ns) is 100 μm wide, and the rectangle marks the approximate incident beam position.

than that parallel to it and this caused the cloud to expand in the direction of the normal to the donor surface. In the time span of t = 250–1300 ns, two initially compact and darker areas were seen in the particle cloud. The one further away from the donor surface travelled with a velocity slightly lower than that of the fastest particles, whereas the area closer to the donor propagated with a velocity estimated to be about three times lower than that of the fastest particles. The effect of separately travelling transfer products has been seen before in LIFT. During transfer of thin metal films with fs-pulses, two plumes travelling at velocities of 300 m/s and 50 m/s were observed [20]. In another publication where the flyer consisted of a bilayer of aluminium and the polymer MEH-PPV, the latter decomposed and was separated from the metal layer during transfer [7]. It could be speculated that at high fluence, the molten, highly energetic particles from the vapourised donor volume break through the solid part of the donor and propagate away from the donor surface with high velocity. The solid particles (from nearer the donor surface) cannot gain further momentum other than acquired by impact from some of the fast particles, as the pressure from the isolated and vapourised absorption volume in the donor ceased to act onto these solid but fragmented particles as during the initial phase after absorption of the laser pulse. Kaur et al. [21] on the other hand reported debris from the edges travelling at a slower velocity then the ejected flyer. Eventually we cannot exclude one explanation for the other.

Another feature that the images reveal is a specific time lag of material ejection which decreases for increasing fluence. This phenomenon could be explained by a faster pressure build-up at the donor/carrier interface when using a higher fluence. Moreover, the early material removal at high fluences can be the result of an explosive eruption of material where the vapourised material acquires energy high enough to drive through the still solid part of the flyer. For the case of a flyer in an intact state, material ejection does not start earlier than with the acceleration of the flyer, which due to its increased mass experiences a smaller acceleration than the small fragmented particles in the case of an ejection at high fluence.

The divergence of the particle cloud was determined by the cloud's slowest particles which were observed at t = 1300 ns within a cone angle of 55°. The fastest particles were concentrated next to the normal to the donor surface and hence did not further contribute to the spread of the particle cloud. This led to the cloud forming a pyramid-like shape above the target as seen in the frames at time intervals of 200–1000 ns in Fig. 3. For times larger than 1300 ns the fastest particles started to travel beyond the observed frame. Nevertheless, slow particles were still seen at a camera delay time of 10 μs.

The velocity of a flyer was found by linearly fitting the data points for the flyer propagation distance versus the camera delay time. As reported before [21] there was some material that was released around the peripheral region of the flyer which moved separately from the main part of the material. Intact flyers were observed in about 50% of the cases for fluences of ~90–130 mJ/cm^2 within an imaged field of up to 500 μm over which the flyer's propagation velocity appeared to remain constant. Fig. 4 shows a plot of the distance travelled by a flyer from a bismuth selenide donor versus time.

The plots in Fig. 4 are for three different values of laser fluence at the interface of carrier and donor. As a reference the speed of sound in standard air (331.3 m/s [22]) is drawn as a dashed line. For fluences above ~130 mJ/cm^2, flyers fragmented into several particles.

In case of solid transfer achieved for ~90 mJ/cm^2 and ~130 mJ/cm^2, the flyer velocities were deduced as 48 ± 7 m/s and 65 ± 10 m/s respectively. As seen in Table 1, as expected, the velocity of an intact flyer increased with fluence.

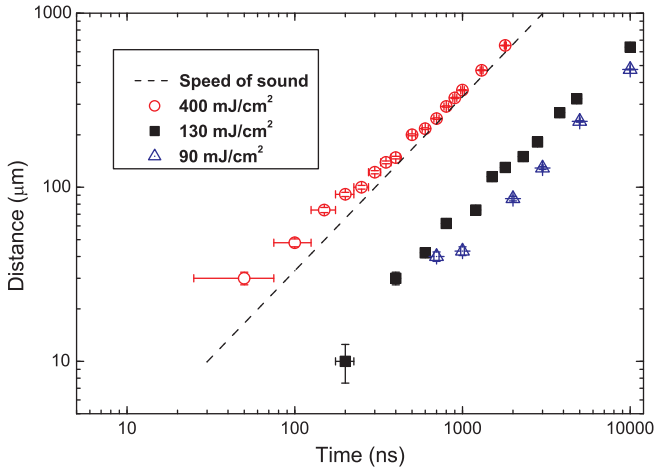

Fig. 4. Plot of Bi_2Se_3 flyer or fastest particle distance versus time. For comparison the speed of sound in air (331.3 m/s) is drawn as the thick dashed line.

The values in Table 1 are particle velocities that were deduced from a linear fit of the velocity of the fastest particles for times larger than 1 μs or for a flyer in case of intact transfer. The time delay of 1 μs was chosen deliberately within the set of complete data and as only values for a delay of larger than 0.7 μs were available for all the plots, we have chosen this next nearest larger value of 1 μs.

As seen in Fig. 4, the fastest ejected particles exceeded the speed of sound in air for a laser fluence of ~400 mJ/cm^2 and had a velocity of 354 ± 12 m/s. Similarly, for conditions that created a fragmented flyer during LIFT, velocities of ~365 m/s have been seen in other sub-picosecond LIFT experiments [13].

3.2. PZT

A crucial point for establishing LIFT as a tool for micro fabrication is the reliability of the transfer process for various material types and thicknesses. In order to validate this we attempted to LIFT PZT which is a widely used piezoelectric material. Material with a thickness of 1.8 μm was transferred around a threshold of ~360 mJ/cm^2. The much higher threshold fluence value required for transfer as compared to that for bismuth selenide can be readily associated with the different donor growth conditions and layer thickness.

The temporal evolution of the transfer of a compact flyer is shown in Fig. 5.

Fig. 5 shows shadowgraph images of PZT LIFT at a fluence of ~360 mJ/cm^2, taken at varying delay times which are shown below each frame. The PZT flyer started to emerge from the donor surface after a camera delay time of about 50–100 ns. Throughout the selected frames that were all imaged from different LIFT events, the flyers were not found to travel in a stable orientation relative to their own axis. Due to tilt the flyer appeared to be thicker than the actual donor in some cases. In other cases, such as after 6000 ns (Fig. 5), one side of the flyer travelled a lesser distance than its corresponding opposite side. The different frames were chosen in order to illustrate the tilting of the flyer. We assume that this may

Table 1
Velocity of fastest particle from a fragmented flyer or velocity of intact flyer for transfer of Bi_2Se_3 at different laser fluences. The value shown is a fit to the velocity for times larger than 1 μs.

Laser fluence (mJ/cm^2)	Velocity (m/s)	Flyer integrity
~90	~48 ± 7	Intact
~130	~65 ± 10	Intact
~400	~354 ± 12	Fragmented

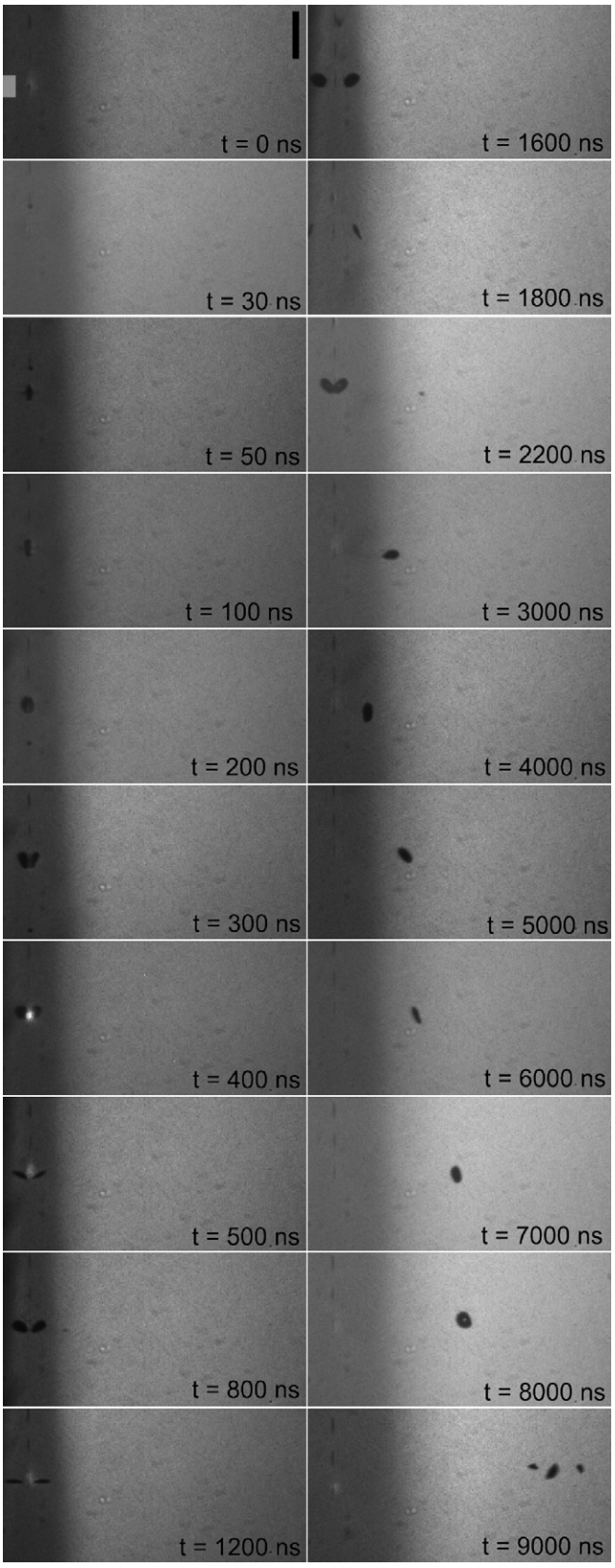

Fig. 5. Shadowgraph images of a PZT flyer transferred by fs-LIFT. The scale in the first frame ($t = 0$ ns) is 100 μm wide. The rectangle in the same frame sketches the vertical position of the absorbed beam and hence the origin of the flyer. In some frames (i.e. at $t = 2200$ ns) it is possible to see the mirror image of the flyer reflected from the donor surface below. The transfer fluence was ~360 mJ/cm^2.

be caused by slight variations in the morphological homogeneity of the donor, as well as the spatial non-uniformity of the LIFTing laser pulse. This emphasises the importance of the use of a small spacing between the receiver and the target during fs-LIFT. Typically, the receiver is placed at a maximum distance of a few microns from the donor surface so such tilting or spinning would not present much of a problem.

To study the repeatability of intact transfer over a large travelled distance, we repeatedly took images at a fixed delay time of 10 μs for different transferred flyers. In about half of the cases, the flyer was still intact at a delay of 10 μs. We assume that the flyer either broke or remained intact due to slight variations in laser or donor conditions as mentioned above. The different transfer behaviour at different donor positions for the same delay time and identical laser conditions are seen in Fig. 6.

Fig. 6 shows six examples of different shadowgraph images capturing six different flyers for identical delay times and laser conditions. Flyers were either intact and tilted (frames 1 and 5 of Fig. 6), or they broke into several fragments which travelled with different velocities relative to each other (frames 2–4 and frame 6 in Fig. 6). However, although appearing to be slightly tilted, the intact flyers travelled a similar distance which was important for the reliability and accuracy of the propagation measurements. Another important observation was that besides their orientation they were travelling in the same straight line normal to the donor surface. Fragmented particles were not considered in the calculation of flyer distances.

The results of the shadowgraph experiments that were carried out with a fluence of ~720 mJ/cm^2 that did not result in intact transfer are seen in Fig. 7.

The shadowgrams show the transfer events for LIFT with a fluence which was about two times the threshold value. Here, the first material removal started after 20 ns. However it can be clearly seen that material ejection took place earlier than that for LIFT at threshold fluence (~360 mJ/cm^2). During this non-intact transfer, after ~50 ns, the flyer that was released from the target surface appears fragmented. As seen in the images for times larger than 100 ns, there is a part of the fragments in the centre that travelled faster than the main particle cloud. Just as in the case of a Bi_2Se_3 flyer, for PZT, this led to the formation of two particle clouds which were clearly observable in the time span of 200–800 ns. It was observed earlier that the spatial distribution of material removal was not homogeneous, as the fastest particles possessed a larger propagation velocity in the direction of the incident laser beam path than in the direction orthogonal to it [23].

The analysis of the temporal evolution of the flyer revealed a flyer velocity of ~34 ± 5 m/s for a fluence of ~360 mJ/cm^2. As seen earlier (Figure 4) for bismuth selenide, for PZT a higher fluence resulted in a transfer of a fragmented flyer with particles that travelled at velocities that depended on the laser fluence, as seen in Fig. 8.

Fig. 8 shows the distance travelled by a flyer from a PZT donor layer versus time. As a reference the speed of sound in standard air is drawn as a dashed line.

The measurements show, as expected, that the velocity of the fastest particle increased with laser fluence, from ~147 m/s for ~435 mJ/cm^2 up to a value of ~360 m/s for ~720 mJ/cm^2. The fitted velocity of a flyer approached an almost constant value which is shown in Table 2.

As we can see, the velocity of a PZT flyer transferred at a fluence regime above transfer threshold was lower (~34 m/s) compared to the flyer velocity of a thinner layer of Bi_2Se_3 (~48 m/s) LIFTed in the same regime. With the help of Eq. (1) we can estimate the kinetic energy E_{kin} of both flyers to be ~4.5×10^{-9} J.

$$E_{kin} = \frac{1}{2} A d \rho v^2 \quad (1)$$

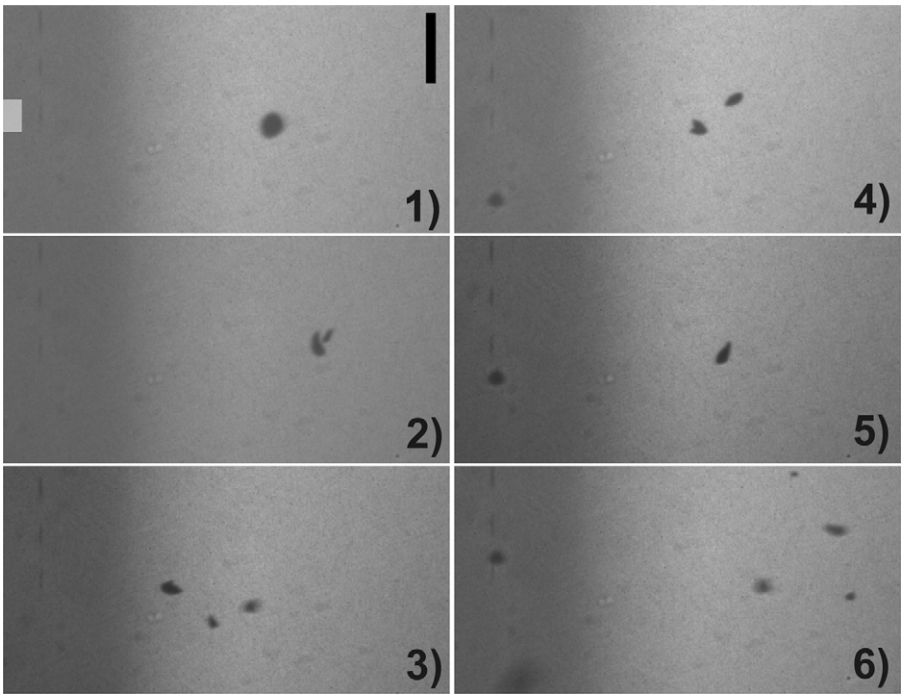

Fig. 6. Shadowgraph of LIFT of a PZT flyer for a fixed camera delay time of 10 μs. Each frame represents a different transfer event with all other conditions remaining constant. The scale bar in the first frame is 100 μm wide, and the rectangle in the same frame indicates the approximate vertical position of the beam.

where A is the cross-section of the flyer, d is the donor thickness, ρ is the density of the donor and v is the velocity of the flyer.

We have, of necessity, neglected the unknown amount of debris and exact layer composition contributing to an uncertainty in estimating the mass and density of the flyers. At transfer threshold for PZT the laser delivered an energy E_{laser} of $\sim 2 \times 10^{-6}$ J which was about 450 times the flyer's kinetic energy.

Thus just a small amount of laser energy was actually used for the propulsion of the flyer. Furthermore, even though the threshold fluence of the two different materials differed by a factor of four, the amount of energy that is transferred into the propulsion of the flyer remained roughly the same. This means that additional factors such as layer thickness and the specific material properties contribute more to the determination of a material's transfer threshold rather than just the mass of a LIFTed flyer.

At this stage it is difficult to present a more detailed explanation about the dependence of flyer velocity on the laser fluence as it would need further study on the proportion of the laser energy actually used to propel the flyer or particles forward, and the energy fraction needed for the phase transition and/or decomposition of the ejected material. A detailed study that describes the energy balance for ns-LIFT can be found in [24].

3.3. Terfenol-D

For the magnetostrictive alloy Terfenol-D we investigated the behaviour of transfer around its threshold fluence of ~145 mJ/cm^2 and for a higher value of ~460 mJ/cm^2. The donor layer had a thickness of ~500 nm. Just above threshold, we found that the flyer was either transferred intact (Fig. 9(a)) or in a fragmented state (Fig. 9(b)). The fragments were smaller in size than the diameter of the ablated spot on the donor, as seen in Fig. 9.

Table 2
Velocity of fastest particle from a fragmented flyer or velocity of intact flyer for transfer of PZT at different laser fluences. The velocity was calculated by a fit to the fastest particle or the intact flyer visible on the shadowgraph image after 1 μs.

Laser fluence (mJ/cm^2)	Fastest particle velocity (m/s)	Flyer integrity
~360	34 ± 5	Intact
~435	147 ± 10	Fragmented
~720	360 ± 15	Fragmented

The repeatability of transfer with a flyer in an intact state was low. For a fluence of 10% above threshold we saw decomposition of the flyer during transfer in all cases. This meant that for this donor the fluence window for compact transfer was much narrower than for PZT and Bi_2Se_3. As seen in Fig. 10, the transfer behaviour at high fluence was qualitatively similar to a transfer of liquid donors [25].

Up to a delay time of about 50–100 ns, a hemispherical bubble made of donor material formed above the donor. Later the bubble broke up and fast particles were ejected from its centre. Due to this behaviour the deposit was expected to be transferred in a molten state when compared to the largely solid matter that was ejected with fluences around the threshold fluence for this, and the previously discussed materials. The transfer behaviour shows similarity to a regime described by Young et al. [18] who reported the existence of a plume regime for transfer of fluids at high fluences.

For each of the image sequences taken, we calculated the velocity of the fastest particle. Transfer above threshold range resulted in a blast wave of material wherein the fastest particles travelled at velocities that increase with laser fluence. For a fluence of ~460 mJ/cm^2 for instance, we measured particle velocities as high as ~562 m/s. As a comparison, the flyer for fluences around threshold travelled at ~140 m/s. This velocity was higher than that observed for the thicker layers of Bi_2Se_3 and PZT under similar transfer conditions and thus followed the propagation characteristics described in Sections 3.1 and 3.2.

3.4. Implications for LIFT

The flyer velocities observed for our LIFT experiments around the threshold fluence were to the best of our knowledge well below those observed so far for any other intact flyers, in other LIFT studies. Low ejection velocities during LIFT have been reported before, but neither was the flyer intact, nor was the event captured in an

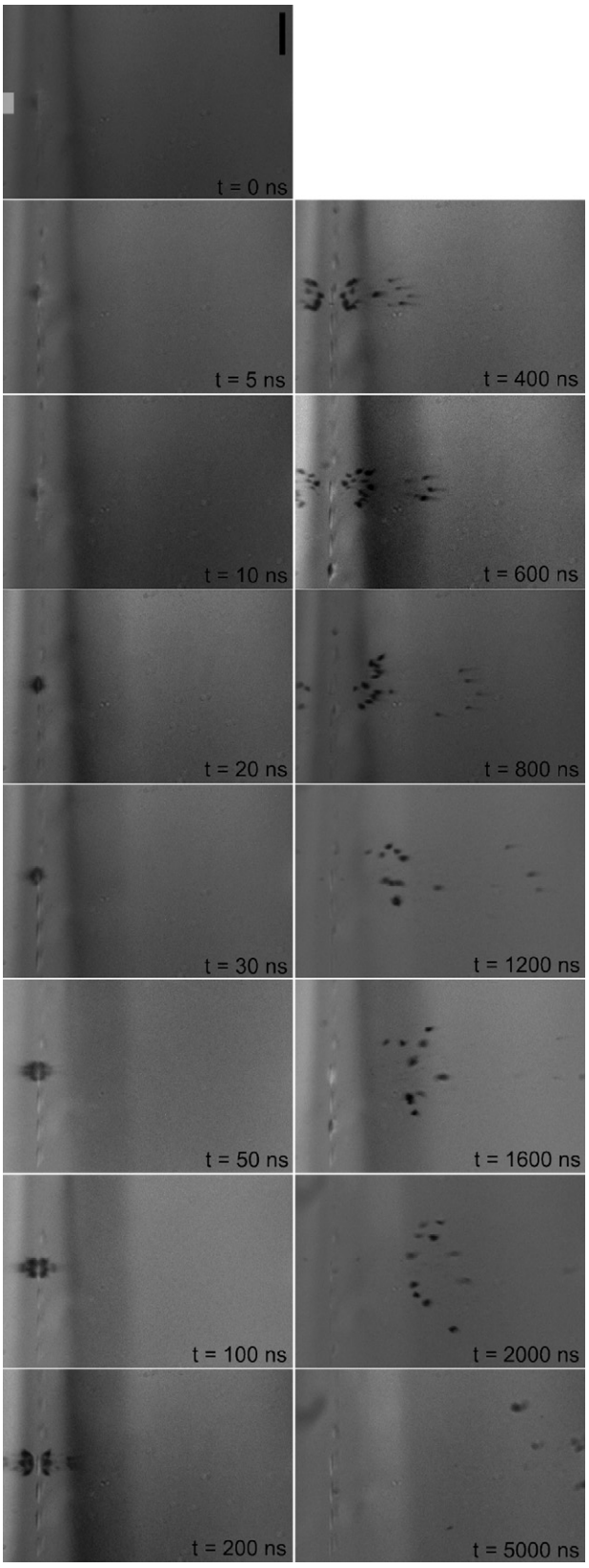

Fig. 7. Shadowgraph images of a PZT flyer transferred by fs-LIFT. The scale bar in the first frame (t = 0 ns) is 100 μm wide, and the rectangle sketches the approximate incident beam position. In some frames it is possible to see the mirror image of the flyer on the donor surface below. The transfer fluence is ~720 mJ/cm^2.

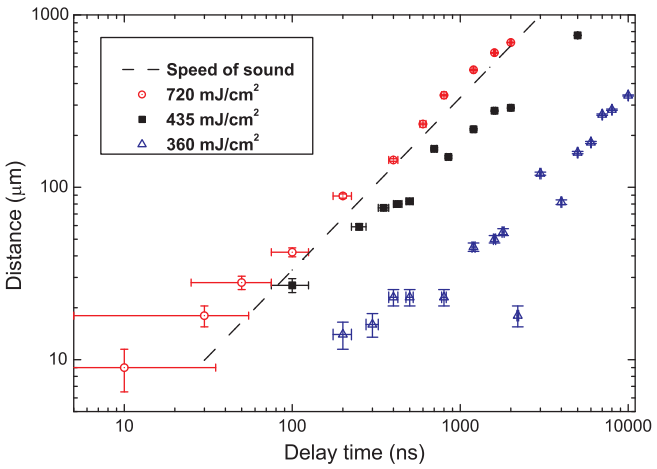

Fig. 8. Plot of distance travelled by PZT flyer and fastest particle versus time. For comparison the speed of sound (331.3 m/s) is drawn as a dashed line. Solid transfer at fluence of ~360 mJ/cm^2 and fragmented transfer for fluences of ~435 mJ/cm^2 and higher is shown.

image [26]. Work carried out by laser-induced assembly showed flyer velocities in the range of ~0.1–50 m/s, where the flyers consisted of electronic dies that were attached to a support ribbon prior to transfer [27,28]. In experiments with blister-actuated LIFT of powders and liquids, similar velocities were observed in low fluence regimes for the slowest particles [17,29]. However, transfer of solid, 0.2–1 μm thick donor material in the nanosecond [20,30] and sub-picosecond regime (~500 fs) [14] showed flyers with a higher propagation speed than reported here. Flyer velocity is clearly a function of donor thickness and depends on the use of a DRL layer.

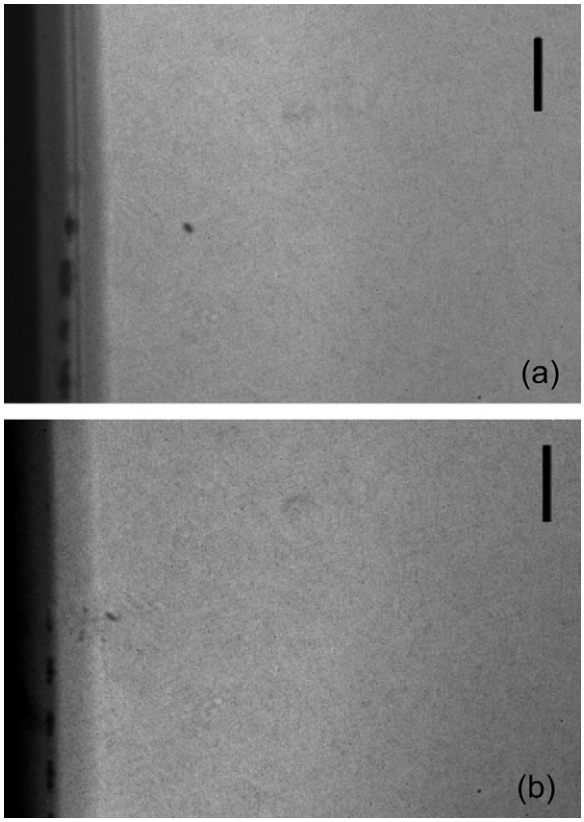

Fig. 9. Transfer of Terfenol-D at threshold fluence of ~145 mJ/cm^2. The camera delay times were (a) 1 μs and (b) 500 ns. The scale bar in each figure is 100 μm wide.

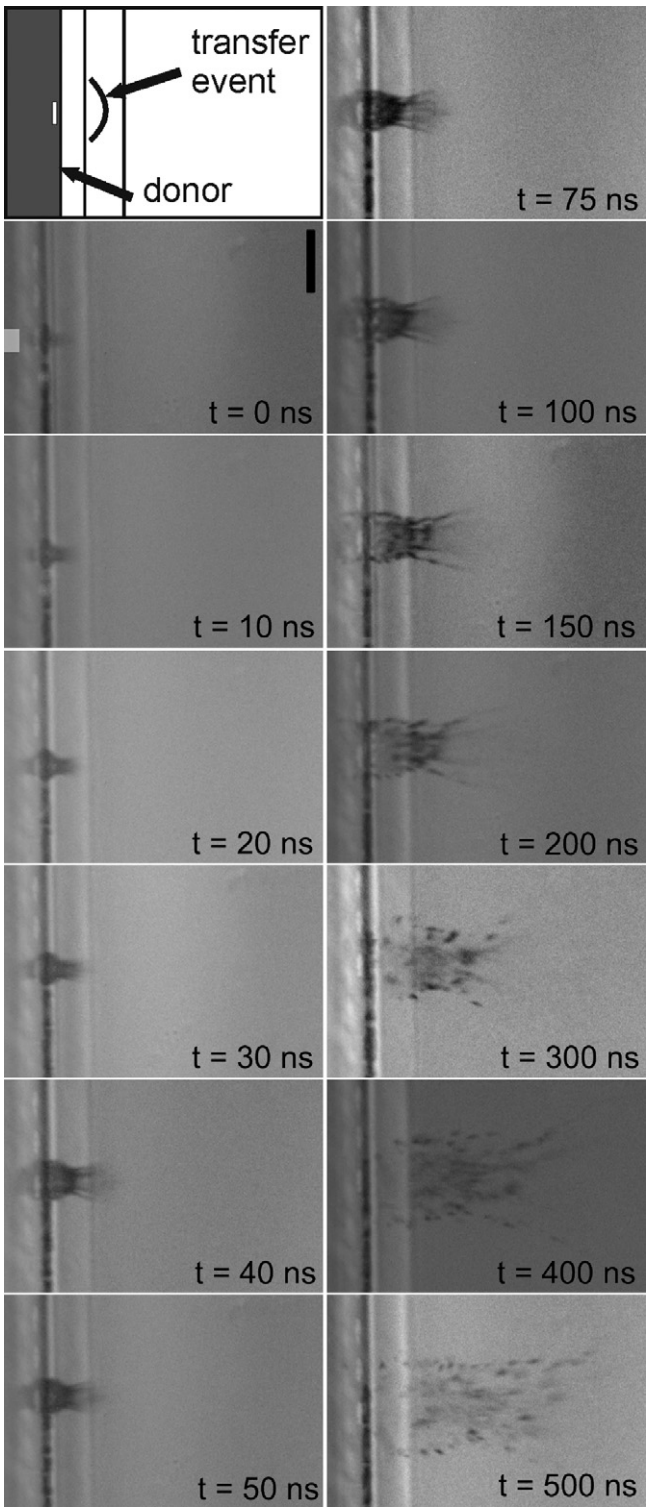

Fig. 10. Surface of Terfenol-D donor after varying camera delays of 0–500 ns after the absorption of the femtosecond laser pulse arriving from the side marked by the rectangle in the first frame (t = 0 ns). The scale bar in the same frame is 100 μm wide. The transfer fluence was ~460 mJ/cm^2.

It is of particular importance to preserve the integrity of the transferred flyer for successful LIFT. A high kinetic energy increases the flyer's impact on the receiver. This impact energy in turn is responsible for possible breaking of the intact flyer when arriving at the receiver. A lower velocity of the flyer also implies that less drag (drag is proportional to the square of the velocity) is acting on the flyer which further decreases the possibility of flyer decomposition during transfer. We can say that the higher the kinetic energy, the higher the chance that drag or impact forces exceed the forces preserving the integrity of the flyer.

For our ~0.5–1.8 μm thick donors, images showing the donor surface for transfer with a fluence just above threshold did not show any trace of shock wave propagation spreading from the impacted region. In time-resolved studies of LIFT so far this phenomenon was clearly visible throughout the observed laser fluences [7,20]. Fardel et al. [7] indicated that this shock wave may interact destructively with the flyer when reflected from the receiver which may result in unsuccessful transfer. It could be argued that the shock wave results solely from the use of an auxiliary decomposing polymer layer used in many LIFT experiments [12]. In contrast however it has been observed [31] that a shock wave was created even by local ablation at an interface of two material layers without such an explosive layer. The authors also argue that the shock wave transmitted into the area beyond the donor surface is much weaker than the one reflected from the auxiliary foil/air interface due to a strong acoustic impedance mismatch. Zeng [23] imaged the ablation phenomena for fs and ns laser pulses (wavelength 266 nm) and could distinguish qualitative differences in the dynamics of the shock wave, namely the fast decrease of electron density and plasma temperature for fs-pulses compared to the ns-case. We assume that in our study the laser energy density was too low to create an observable shock wave from impact as was reported in other studies [32,33].

For laser-induced forward transfer it is vital to avoid the creation of a shock wave as it is a possible cause for the destruction of the flyer.

In our experiments, we believe that the low flyer speed, the non-inclusion of a decomposing dynamic release layer and the high acoustic impedance at the flyer(donor)/air interface contributed to the absence (or reflection) of any observable blast or shock wave preceding or lagging the transferring flyer using this shadowgraphy technique.

As the main objective of LIFT is to transfer material in an intact state, it is of crucial importance to decrease or eliminate factors, such as high velocity and the presence of a shock wave, which would oppose the ability and reliability of successful transfer of these materials.

4. Conclusions

In our studies we have observed by shadowgraphic imaging the transfer of solid material that remained intact during the LIFT process. Furthermore we have identified conditions under which the transferred flyer was molten or fragmented. The intact flyers travelled at a lower velocity than that previously observed in ns- or ps-LIFT of solid materials. Additionally, we could not identify a shock wave during our experiments. This indicates that fs-LIFT of thick donor films without a dynamic release layer could be appropriate for printing solid and intact material under atmospheric conditions when compared to other LIFT techniques.

In summary, we report the first shadowgraph imaging of femtosecond laser-induced forward transfer of intact solid thin films. The flyer velocity detected in a low fluence regime was as low as ~34 m/s which was lower than those ever reported before in solid transfer by ns- and ps-LIFT. The identification of a regime for intact transfer with low flyer speed is important to understand the adhesion and transfer quality seen in femtosecond LIFT so far [13,34].

Acknowledgements

The research leading to these results has received funding from LASERLAB-EUROPE (grant agreement no. 228334, EC's

Seventh Framework Programme, proposal: cnrs-lp3001685) and from the e-LIFT project (no. 247868-FP7-ICT-2009-4) which are greatly acknowledged. Thanks also go to Behrad Gholipour and Fabio Di Pietrantonio for preparation of the Bi_2Se_3 and the PZT samples respectively.

References

[1] D. Toet, M.O. Thompson, P.M. Smith, P.G. Carey, T.W. Sigmon, Thin film transistors fabricated in printed silicon, Japanese Journal of Applied Physics 38 (1999) L1149–L1152.
[2] R. Wartena, A.E. Curtright, C.B. Arnold, A. Pique, K.E. Swider-Lyons, Li-ion microbatteries generated by a laser direct-write method, Journal of Power Sources 126 (2004) 193–202.
[3] S. Mailis, I. Zergioti, G. Koundourakis, A. Ikiades, A. Patentalaki, P. Papakonstantinou, N.A. Vainos, C. Fotakis, Etching and printing of diffractive optical microstructures by a femtosecond excimer laser, Applied Optics 38 (1999) 2301–2308.
[4] B.R. Ringeisen, D.B. Chrisey, A. Pique, H.D. Young, R. Modi, M. Bucaro, J. Jones-Meehan, B.J. Spargo, Generation of mesoscopic patterns of viable *Escherichia coli* by ambient laser transfer, Biomaterials 23 (2002) 161–166.
[5] M. Duocastella, J.M. Fernandez-Pradas, P. Serra, J.L. Morenza, Laser-induced forward transfer of liquids for miniaturized biosensors preparation, Journal of Laser Micro Nanoengineering 3 (2008) 1–4.
[6] C.B. Arnold, P. Serra, A. Pique, Laser direct-write techniques for printing of complex materials, MRS Bulletin 32 (2007) 23–31.
[7] R. Fardel, M. Nagel, F. Nuesch, T. Lippert, A. Wokaun, Laser-induced forward transfer of organic LED building blocks studied by time-resolved shadowgraphy, Journal of Physical Chemistry C 114 (2010) 5617–5636.
[8] W.A. Tolbert, I.Y.S. Lee, M.M. Doxtader, E.W. Ellis, D.D. Dlott, High-speed color imaging by laser-ablation transfer with a dynamic release layer – fundamental mechanisms, Journal of Imaging Science and Technology 37 (1993) 411–422.
[9] B.N. Chichkov, C. Momma, S. Nolte, F. vonAlvensleben, A. Tunnermann, Femtosecond, picosecond and nanosecond laser ablation of solids, Applied Physics A: Materials Science & Processing 63 (1996) 109–115.
[10] K.S. Kaur, M. Feinaeugle, D.P. Banks, J.Y. Ou, F. Di Pietrantonio, E. Verona, C.L. Sones, R.W. Eason, Laser-induced forward transfer of focussed ion beam premachined donors, Applied Surface Science 257 (2011) 6650–6653.
[11] M. Duocastella, J.M. Fernandez-Pradas, P. Serra, J.L. Morenza, Jet formation in the laser forward transfer of liquids, Applied Physics A: Materials Science & Processing 93 (2008) 453–456.
[12] R. Fardel, M. Nagel, F. Nuesch, T. Lippert, A. Wokaun, Shadowgraphy investigation of laser-induced forward transfer: front side and back side ablation of the triazene polymer sacrificial layer, Applied Surface Science 255 (2009) 5430–5434.
[13] I. Zergioti, D.G. Papazoglou, A. Karaiskou, N.A. Vainos, C. Fotakis, Laser microprinting of InO*x* active optical structures and time resolved imaging of the transfer process, Applied Surface Science 197-198 (2002) 868–872.
[14] D.G. Papazoglou, A. Karaiskou, I. Zergioti, C. Fotakis, Shadowgraphic imaging of the sub-ps laser-induced forward transfer process, Applied Physics Letters 81 (2002) 1594–1596.
[15] A. Bullock, P. Bolton, Laser-induced back ablation of aluminum thin films using picosecond laser pulses, Journal of Applied Physics 85 (1999) 460–465.
[16] Y. Nakata, T. Okada, Time-resolved microscopic imaging of the laser-induced forward transfer process, Applied Physics A: Materials Science & Processing 69 (1999) S275–S278.
[17] T.V. Kononenko, P. Alloncle, V.I. Konov, M. Sentis, Shadowgraphic imaging of laser transfer driven by metal film blistering, Applied Physics A: Materials Science & Processing 102 (2010) 49–54.
[18] D. Young, R.C.Y. Auyeung, A. Pique, D.B. Chrisey, D.D. Dlott, Plume and jetting regimes in a laser based forward transfer process as observed by time-resolved optical microscopy, Applied Surface Science 197–198 (2002) 181–187.
[19] J. Bonse, S.M. Wiggins, J. Solis, T. Lippert, Phase change dynamics in a polymer thin film upon femtosecond and picosecond laser irradiation, Applied Surface Science 247 (2005) 440–446.
[20] A.P. Alloncle, R. Bouffaron, J. Hermann, M. Sentis, Experimental study of front and back ablation of metal thin film using ultrashort laser pulses – article no. 626127, in: C.R. Phipps (Ed.), High-Power Laser Ablation VI, Pts 1 and 2, 2006, p. 26127.
[21] K.S. Kaur, R. Fardel, T.C. May-Smith, M. Nagel, D.P. Banks, C. Grivas, T. Lippert, R.W. Eason, Shadowgraphic studies of triazene assisted laser-induced forward transfer of ceramic thin films, Journal of Applied Physics 105 (2009) 113119.
[22] G.S.K. Wong, Speed of sound in standard air, Journal of the Acoustical Society of America 79 (1986) 1359–1366.
[23] X. Zeng, X.L. Mao, R. Greif, R.E. Russo, Experimental investigation of ablation efficiency and plasma expansion during femtosecond and nanosecond laser ablation of silicon, Applied Physics A: Materials Science & Processing 80 (2005) 237–241.
[24] R. Fardel, M. Nagel, F. Nuesch, T. Lippert, A. Wokaun, Energy balance in a laser-induced forward transfer process studied by shadowgraphy, Journal of Physical Chemistry C 113 (2009) 11628–11633.
[25] P. Serra, M. Duocastella, J.M. Fernandez-Pradas, J.L. Morenza, Liquids microprinting through laser-induced forward transfer, Applied Surface Science 255 (2009) 5342–5345.
[26] K. Alti, A. Khare, Generation of cold low divergent atomic beam of indium by laser ablation, Review of Scientific Instruments 76 (2005) 113302.
[27] N.S. Karlitskaya, J. Meijer, D.F. de Lange, H. Kettelarij, Laser propulsion of microelectronic components: releasing mechanism investigation – article no. 62612P, in: C.R. Phipps (Ed.), High-Power Laser Ablation VI, Pts 1 and 2, Spie-Int Soc Optical Engineering, Bellingham, 2006, pp. 62612-1–62612-10.
[28] A. Pique, N.A. Charipar, R.C.Y. Auyeung, H. Kim, S.A. Mathews, Assembly and integration of thin bare die using laser direct-write – article no. 645802, in: C.B. Arnold, T. Okada, M. Meunier, A.S. Holmes, B. Geohegan, F. Trager, J.J. Dubowski (Eds.), Photon Processing in Microelectronics and Photonics VI, 2007, p. 645802.
[29] M.S. Brown, N.T. Kattamis, C.B. Arnold, Time-resolved study of polyimide absorption layers for blister-actuated laser-induced forward transfer, Journal of Applied Physics 107 (2010) 083103.
[30] L. Rapp, C. Cibert, A.P. Alloncle, P. Delaporte, S. Nenon, C. Videlot-Ackermann, F. Fages, Comparative time resolved shadowgraphic imaging studies of nanosecond and picosecond laser transfer of organic materials, in: R. Vilar, O. Conde, M. Fajardo, L.O. Silva, M. Pires, A. Utkin (Eds.), XVII International Symposium on Gas Flow, Chemical Lasers, and High-Power Lasers, Spie-Int Soc Optical Engineering, Bellingham, 2009, p. 71311L.
[31] V. Menezes, K. Takayama, A. Gojani, S. Hosseini, Shock wave driven microparticles for pharmaceutical applications, Shock Waves 18 (2008) 393–400.
[32] A. Salleo, F.Y. Genin, M.D. Feit, A.M. Rubenchik, T. Sands, S.S. Mao, R.E. Russo, Energy deposition at front and rear surfaces during picosecond laser interaction with fused silica, Applied Physics Letters 78 (2001) 2840–2842.
[33] J.P. McDonald, S.W. Ma, T.M. Pollock, S.M. Yalisove, J.A. Nees, Femtosecond pulsed laser ablation dynamics and ablation morphology of nickel based superalloy CMSX-4, Journal of Applied Physics 103 (2008) 093111.
[34] D.P. Banks, Femtosecond laser induced forward transfer techniques for the deposition of nanoscale, intact, and solid-phase material, PhD thesis University of Southampton, Optoelectronics Research Centre, 2008.